Communication

Commercial P-Channel Power VDMOSFET as X-ray Dosimeter †

Goran S. Ristić [1,*] **, Stefan D. Ilić** [1,2] **, Sandra Veljković** [1] **, Aleksandar S. Jevtić** [1] **, Strahinja Dimitrijević** [1] **, Alberto J. Palma** [3] **, Srboljub Stanković** [4] **and Marko S. Andjelković** [5]

[1] Faculty of Electronic Engineering, University of Niš, 18000 Nis, Serbia; stefan.ilic@nanosys.ihtm.bg.ac.rs (S.D.I.); sandra.veljkovic@elfak.rs (S.V.); aleksandar.jevtic@elfak.rs (A.S.J.); strax.dimitrijevic@elfak.rs (S.D.)

[2] Center of Microelectronic Technologies, Institute of Chemistry, Technology and Metallurgy, University of Belgrade, 11000 Belgrade, Serbia

[3] Department of Electronics and Computer Technology, University of Granada, 18014 Granada, Spain; ajpalma@ugr.es

[4] Department of Radiation and Environmental Protection, "Vinča" Institute of Nuclear Sciences, 11000 Belgrade, Serbia; srbas@vin.bg.ac.rs

[5] IHP—Leibniz-Institut für Innovative Mikroelektronik, 15236 Frankfurt, Germany; andjelkovic@ihp-microelectronics.com

* Correspondence: goran.ristic@elfak.ni.ac.rs

† This paper is an extension version of the conference paper: Ristić, G.S.; Jevtić, A.S.; Ilić, S.D.; Dimitrijević, S.; Veljković, S.; Palma, A.J.; Stanković, S.; Andjelković, M.S. Sensitivity of unbiased commercial p-channel power VDMOSFETs to X-ray radiation. In Proceedings of the IEEE 32nd International Conference on Microelectronics (MIEL 2021), Nis, Serbia, 12–14 September 202; pp. 341–344. https://doi.org/10.1109/MIEL52794.2021.9569096.

Abstract: The possibility of using commercial p-channel power vertical double-diffused metal-oxide-semiconductor field-effect transistors (VDMOSFETs) as X-ray sensors is investigated in this case study. In this aspect, the dependence of sensitivity on both the gate voltage and the mean energy for three X-ray beams is examined. The eight gate voltages from 0 to 21 V are applied, and the dependence of the sensitivity on the gate voltage is well fitted using the proposed equation. Regarding X-ray energy, the sensitivity first increases and then decreases as a consequence of the behavior of the mass energy-absorption coefficients and is the largest for RQR8 beam. As the mass energy-absorption coefficients of SiO_2 are not found in the literature, the mass energy-absorption coefficients of silicon are used. The behavior of irradiated transistors during annealing at room temperature without gate polarization is also considered.

Keywords: VDMOSFETs; X-ray; irradiation; sensitivity; fading

1. Introduction

The idea of using p-channel metal-oxide-semiconductor field-effect transistor (MOSFET), or shorter MOS transistor, as a pMOS dosimeter of ionizing radiation is very old [1], and the basic concept of pMOS dosimeter is to convert the threshold voltage shift, ΔV_T, induced by irradiation, into absorbed radiation dose, *D*. The pMOS dosimeter advantages, in comparison with other dosimetric systems, include immediate, non-destructive read out of dosimetric information, extremely small size of the sensor element, the ability to permanently store the absorbed dose, wide dose range, very low power consumption, compatibility with microprocessors, and competitive price (especially if cost of the read-out system is taken into account). The disadvantages are a need for calibration in different radiation fields ("energy response"), relatively low resolution (starting from about 1 rad), and nonreusability.

Power MOSFETs attract attention when they are stressed by electric fields [2,3], when they are operating in ionizing radiation fields [4–8], and as potential gamma radiation dosimeters [9–11]. Otherwise, many applications of power MOSFETs need to be radiation-hardened [12]. In addition, the influence of ionizing radiation on some MOSFETs con-

taining different materials [13–19] and on some commercial electronic devices [20–22] has been investigated.

There are many investigations of the effect of gamma radiation [9,10,23], protons [5,23], and heavy-ions [6,24] but not the effect of X rays on commercial MOSFETs, to the best of our knowledge. Additionally, their ability to be used as dosimeters of X rays has not been investigated, to our knowledge. X-rays are much more complex and complicated than gamma rays [25] because they are polyenergetic, but the transistor responses are highly dependent on energy from the X-ray spectrum. Many laboratories do not have an X spectrometer but use mean energy and/or a half-value layer as X-beam parameter(s).

In this case study, we investigate the sensitivity, as a main dosimetric parameter, of commercial p-channel VDMOSFETs to X-rays depending on different positive voltages at the gate (a zero gate voltage case was presented in [26]). This transistor type is potentially suitable for radiation dosimetry because it has a relatively thick oxide of about 100 nm. The dependence of sensitivity on X-ray energy is also investigated using three different beam energies. The behavior of densities of positive radiation-induced fixed traps (FTs) in the gate oxide and switching traps (STs) near and at the interface during X-ray irradiation is examined [27,28]. The recovery of the threshold voltage of irradiated transistors during their annealing at room temperature without gate voltage (spontaneous annealing) is also investigated as another dosimetric parameter.

2. Experimental Details

The IRF9520 commercial p-channel VDMOSFETs, mounted in TO-220 plastic packaging, having about 100 nm oxide thickness and pre-irradiation threshold voltage of V_{T0} = 2.9 V, were used. The transistors were irradiated at room-temperature with X-rays to the value of the air kerma of K_{air} = 50 Gy at the Vinča Institute of Nuclear Science, Belgrade, Serbia (a Hopewell Design Beam Irradiator model x80-225 was used). The voltages at the gate during irradiation were $V_{G,irr}$ = 0 V, 3 V, 6 V, 9 V, 12 V, 15 V, 18 V and 21 V, while the drain and source were grounded (in the case of $V_{G,irr}$ = 0 V, all pins of transistors were grounded).

Air kerma, K_{air}, was measured directly with the dosimetric system containing the PTW UNIDOS Webline electrometer and Exradin A3 ionization chamber. The transistors were irradiated at a distance of 35 cm, but K_{air} was measured at a distance of 50 cm, and then K_{air} was recalculated for a distance of 35 cm using the quadratic law.

Three RQR radiation qualities (RQR3, RQR8, and RQR10) were used. The mean energies were calculated by SpekCalc software that is free of charge for research purposes [29]. The characteristics of X-ray beams, the mean energies and air kerma rates are given in Table 1.

Table 1. The X-ray beam type, tube potential (U_p), tube current (I_p), mean energy (E_{mean}), and air kerma rate (DK_{air}).

X-ray Beam	U_p (kV)	I_p (mA)	E_{mean} (keV)	DK_{air} (mG/s)
RQR3	50	30	32.57	9.28
RQR8	100	30	50.82	26.45
RQR10	150	30	56.70	30.31

During irradiation, an automatic system for measuring the electrical transfer characteristics was used [26,30]. This system contains the custom-made switching and bias unit (SABU) [30], and for these experiments a specially designed printed circuit board with relays (PCBR) [26], in which the eight VDMOSFETs were placed, was implemented. The PCBR is connected with SABU via two DSUB cables—one DSUB-25 is for relay control, and the other DSUB-9 is for transistors biasing. The SABU contains a PIC16F887 microcontroller that communicates with the PC via an FTDI chip. The source-measure unit (Keithley 2400 SMU) is connected to the computer via USB-GPIB interface card. The entire system (SABU, PCBR, and SMU) is controlled by the PC using a custom-written program in C#. The block diagram of experimental setup is displayed in Figure 1.
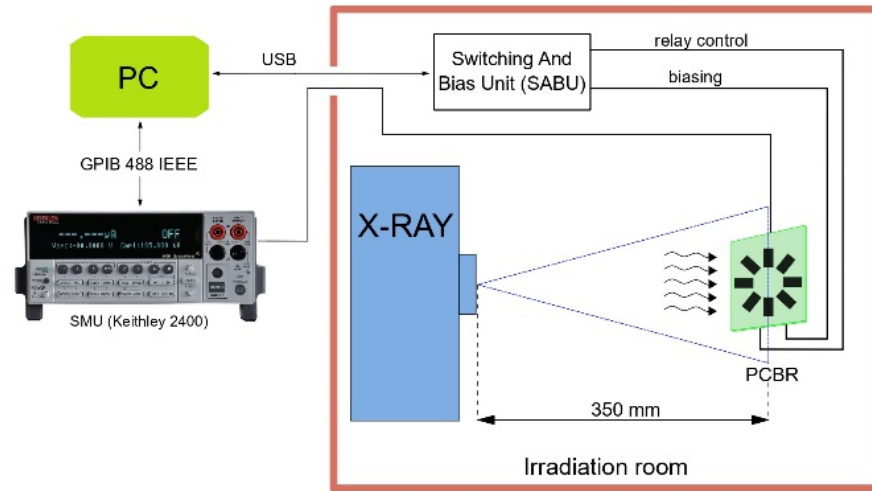
Figure 1. Block diagram of experimental setup.

After irradiation, the spontaneous annealing (SA), representing the room-temperature annealing without a gate voltage ($V_{G,sa}$ = 0 V), was performed up to 3500 h.

The gate and drain were short-connected during the electrical characteristic measurements. The drain-source current, I_{DS}, was forced, and the gate voltage, V_G, was measured. The threshold voltage, V_T, is determined from the electrical transfer characteristics in saturation as the intersection between V_G axis and the extrapolated linear region of the $(I_{DS})^{1/2}$–V_G curves using the least-square method performed in the Octave 6.2.0 program [31]. For p-channel MOSFETs, V_T is negative, but in the whole paper the absolute values of V_T are used.

The threshold voltage shift, ΔV_T, is:

$$\Delta V_T = V_T - V_{T0}. \tag{1}$$

The midgap-subthreshold technique (MGT) that determines the components of ΔV_T of fixed traps (FTs), ΔV_{ft}, and of switching traps (STs), ΔV_{st}, was used [32]. ΔV_T during irradiation and annealing can be presented as:

$$\Delta V_T = \Delta V_{ft} + \Delta V_{st}. \tag{2}$$

Using ΔV_{ft} and ΔV_{st}, the areal densities of FTs, ΔN_{ft} [cm^{-2}], STs, and ΔN_{st} [cm^{-2}], respectively, can be found [32]:

$$\Delta N_{ft} = \frac{C_{ox}}{e} \Delta V_{ft}, \; \rightarrow \; \Delta N_{st} = \frac{C_{ox}}{e} \Delta V_{st}. \tag{3}$$

where $C_{ox} = \varepsilon_{ox}/t_{ox}$ is the gate oxide capacitance per unit area, $\varepsilon_{ox} = 3.45 \times 10^{-13}$ F/cm is the silicon-dioxide permittivity, and e is the electron charge.

Since the MGT is an electrical measurement technique that does not really recognize the physical location of the traps but recognizes the electrical activity of created traps, we usually use ΔN_{ft} and ΔN_{st} as they better reflect the electrical response of the traps, compared to the more commonly used quantities, which imply the physical location of the traps: the density of oxide traps (the traps in the oxide), ΔN_{ot}, and the density of interface states (the states exactly at the SiO$_2$/Si interface), ΔN_{it}.

The traps, created by any stress (radiation, electric fields, temperature, etc.), which do not capture the carriers (charge) from the channel (i.e., do not exchange carriers (charge) with the channel) within the time frame of the electrical MG measurement, represent the FTs. The traps, created by any stress, which capture the carriers (charges) from the channel

(exchange carriers (charges) with the channel) within the time frame of the electrical MG measurement, represent the STs [31].

The STs consist of traps created in the oxide but very near the SiO_2/Si interface, called the slow switching traps (SSTs) or border traps, and of traps created exactly at the SiO_2/Si interface, called fast-switching traps (FSTs), true-interface traps (true interface states), or simply-interface traps (states). The correlation between the densities of these traps is [33]:

$$\Delta N_{st} = \Delta N_{sst} + \Delta N_{fst}, \tag{4}$$

where ΔN_{sst} is the density of SSTs and ΔN_{fst} is the density of FSTs. It is obvious that ΔN_{ot} includes the FTs and SSTs but ΔN_{it} only includes FSTs, and the correlations are $\Delta N_{ot} = \Delta N_{ft} + \Delta N_{sst}$ and $\Delta N_{it} = \Delta N_{st} - \Delta N_{sst} = \Delta N_{fst}$.

3. Results and Discussion

The results of the threshold voltage shift, ΔV_T, during irradiation with $V_{G,irr}$ = 21 V (maximum gate polarization used), for all three X-ray beams, are shown in Figure 2. The case with the minimum value of the gate polarization of $V_{G,irr}$ = 0 V (zero gate polarization) was considered in [26]. All used gate polarizations, including zero gate polarization, show the same behavior.
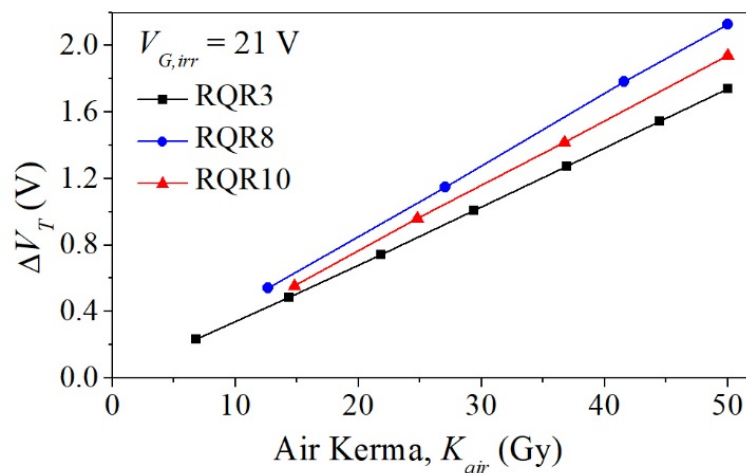

Figure 2. Threshold voltage shift versus air kerma.

It was shown that the dependence of ΔV_T on K_{air} for $V_{G,irr}$ = 0 V is linear up to the investigated air kerma of 50 Gy [26]:

$$\Delta V_T = S \cdot K_{air}, \tag{5}$$

where S is the sensitivity of the transistors to radiation. Linearity is expected to increase with increasing gate polarization. Here, it is proven that the $\Delta V_T = f(K_{air})$ dependence for all used gate polarizations is linear according to Equation (5) (shown only for $V_{G,irr}$ = 21 V in Figure 2), and r-square (r^2) correlation coefficients of linear regression are higher than 0.99 for all cases. Table 2 shows the sensitivity of irradiated VDMOSFETs.

Our investigations have shown that the following simple function can fit very well the dependence of ΔV_T on $V_{G,irr}$, at certain dose [34].

$$\Delta V_T(V_G) = \Delta V_{T,sat}(1 - r \cdot s^{V_{G,irr}}), \tag{6}$$

where $\Delta V_{T,sat}$ is the saturation value of ΔV_T, and r and s are the positive constants.

Table 2. The sensitivity, *S*, of irradiated VDMOSFETs.

V_G (V)	S_{RQR3} (mV/Gy)	S_{RQR8} (mV/Gy)	S_{RQR10} (mV/Gy)
0	6.76	7.78	7.13
3	19.46	22.21	20.50
6	24.10	27.50	25.68
9	28.33	32.18	28.57
12	30.38	34.36	32.28
15	30.27	38.81	35.00
18	33.90	42.91	38.36
21	34.61	42.63	38.33

Consequently, a similar equation can be used to fit the dependence of *S* on $V_{G,irr}$:

$$S(V_G) = S_{sat}(1 - a \cdot b^{V_G,irr}) \, , \tag{7}$$

where S_{sat} is the saturation value of *S*, and *a* and *b* are the positive constants. Figure 3 shows that the fitting of sensitivity using Equation (7) is good. The parameters of Equation (7), obtained as a result of fitting shown in Figure 3, are given in Table 3.
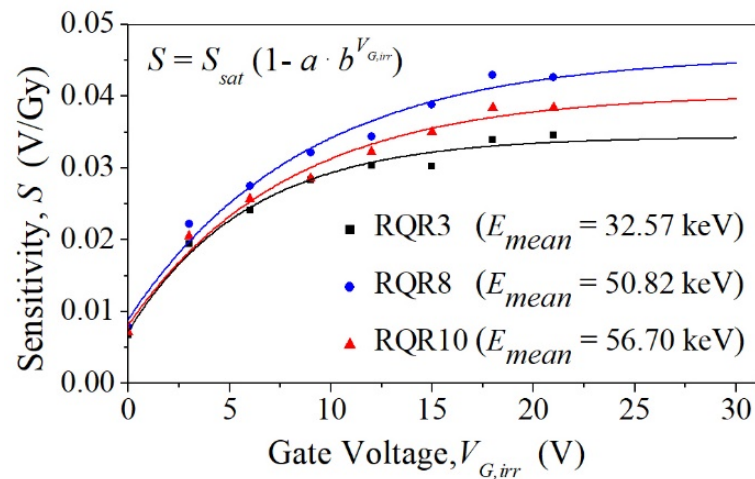

Figure 3. The *S* versus $V_{G,irr}$ fitted by Equation (7).

Table 3. The parameters of Equation (7) for three beams.

X-ray Beam	S_{sat} (mV/Gy)	a	b
RQR3	0.0343	0.7868	0.8447
RQR8	0.0457	0.8040	0.8907
RQR10	0.0403	0.7980	0.8805

The dependence of the density of FTs and ΔN_{ft} on K_{air} for $V_{G,irr}$ = 21 V is shown in Figure 4. ΔN_{ft} is the highest for the RQR8 beam but the lowest for RQR3. ΔN_{ft} also shows this behavior for the other used polarizations (not shown), except for $V_{G,irr}$ = 0 V, analyzed in [26], where ΔN_{ft} is also the highest for the RQR8 beam but almost the same for the other two beams. Figure 5 shows that ΔN_{st} is about 50% less than ΔN_{ft} for $V_{G,irr}$ = 21 V, and ΔN_{st} is the highest for RQR3 and the lowest for RQR10. $V_{G,irr}$ = 0 V shows opposite behavior, and ΔN_{st} is the highest for the RQR10 beam but the lowest for RQR3 [26].
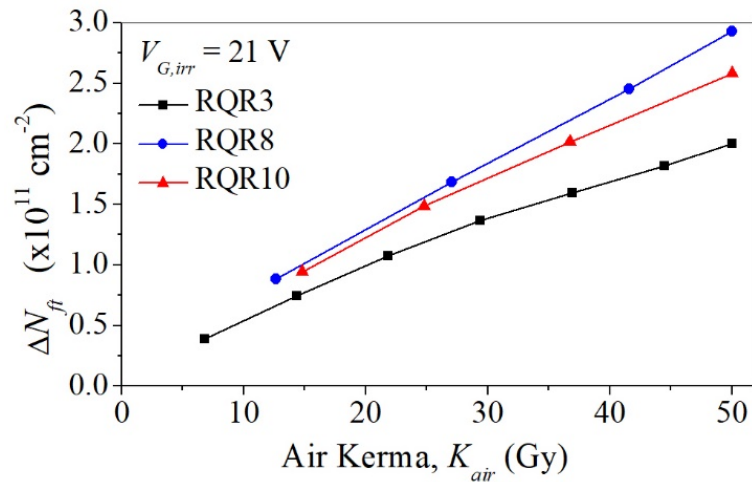
Figure 4. Radiation-induced oxide fixed-trap density versus K_{air}.
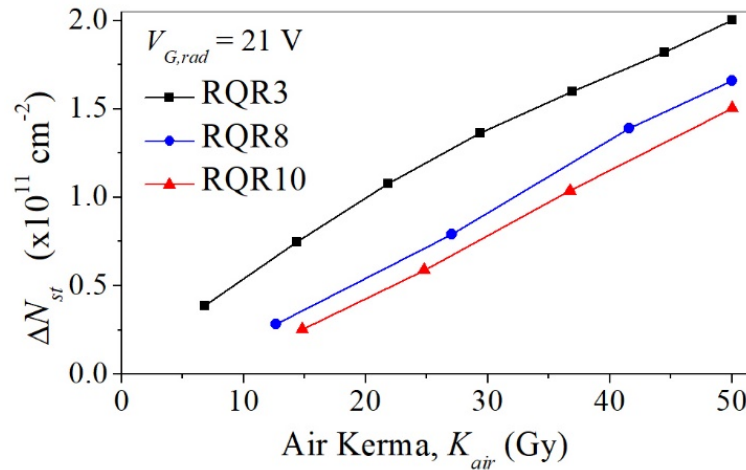

Figure 5. Radiation-induced switching-trap density versus K_{air}.

$\Delta N_{ft} = f(V_{G,irr})$ dependence is not linear, and it is not possible to find a simple parameter similar to sensitivity by which we could easily consider the dependence of ΔN_{ft} on $V_{G,irr}$. Therefore, ΔN_{ft} at a certain K_{air} should be considered, and it is best to take the last point during irradiation, i.e., $K_{air} = 50$ Gy. The same goes for $\Delta N_{st} = f(V_{G,irr})$. The values of ΔN_{ft} at 50 Gy are presented in Figure 6, showing that the highest density is for RQR8 and the lowest for the RQR3 beam. This behavior corresponds to the sensitivity shown in Figure 3. However, ΔN_{st} does not show any clear dependence on $V_{G,irr}$ as ΔN_{ft} (Figure 7). ΔN_{ft} is twice as large as ΔN_{st} and has a more dominant effect on ΔV_T than ΔN_{st}. Although ΔN_{ft} contribution to ΔV_T is still significant, it is much lower than in the case of gamma radiation of VDMOSFETs, when ΔN_{ft} is usually more than five times higher than ΔN_{st} [31,35].
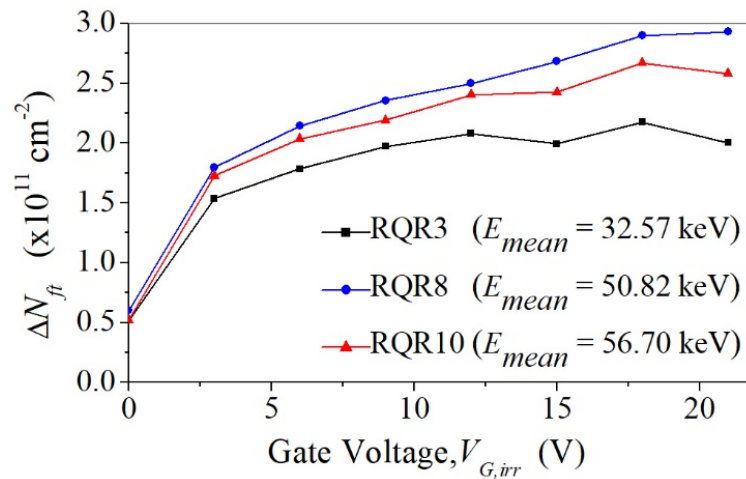
Figure 6. ΔN_{ft} at K_{air} = 50 Gy versus gate voltage during irradiation.
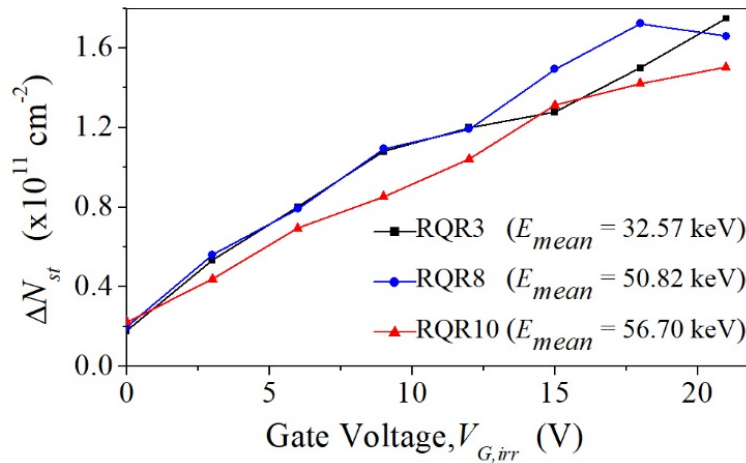

Figure 7. ΔN_{st} at K_{air} = 50 Gy versus gate voltage during irradiation.

Figure 8 shows the dependence of ΔN_{ft} at K_{air} = 50 Gy on mean beam energy, E_{mean}. The behavior is the same for all applied voltages, as in the case of $V_{G,irr}$ = 21 V shown in Figure 4, including zero polarization [26].

The absorbed dose, D, in matter represents the mean energy absorbed per unit mass of irradiated matter at the point of interest, and for a constant incident radiation flux it is defined as follows:

$$D = \frac{E_{ab}}{m} \left(\frac{Gy}{kg} \right),$$ (8)

where E_{ab} is the mean absorbed energy in the matter and m is the mass of the matter. Taking into account the mechanisms of creating traps in the oxide during irradiation [31], it is absolutely clear that ΔN_{ft} depends on the energy absorbed in the gate oxide (SiO_2). Based on Equation (8), it follows that ΔN_{ft} directly depends on the absorbed dose in SiO_2 and D_{SiO2}.

If all X-ray photons have the same energy corresponding to the mean energy, E_{mean}, then only one type of interaction effect will be involved (the photoelectric effect for these mean energies [31]). However, it should be borne in mind that it is a polyenergetic radiation spectrum that also includes radiation photons of lower and higher energies, so for some energies the Compton effect is dominant.
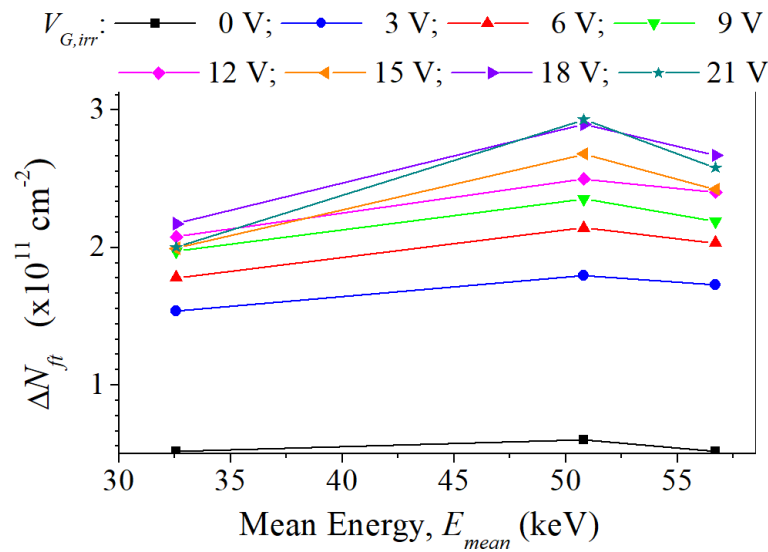
Figure 8. ΔN_{ft} at K_{air} = 50 Gy versus mean beam energy.

The absorbed dose in matter is related to the kerma in air via the equation [31]:

$$D = \frac{(\mu_{me}(E))_{\text{matter}}}{(\mu_{me}(E))_{\text{air}}} K_{air}, \tag{9}$$

where $(\mu_{me}(E))_{\text{matter}}$ and $(\mu_{me}(E))_{\text{air}}$ are the mass energy-absorption coefficients of the matter and air, respectively. These coefficients are energy-dependent, and for SiO_2 Equation (9) can be written as

$$D_{SiO_2} = \frac{(\mu_{me}(E))_{\text{SiO}_2}}{(\mu_{me}(E))_{\text{air}}} K_{air}, \tag{10}$$

where $(\mu_{me}(E))_{\text{SiO2}}$ represents the mass energy-absorption coefficients of SiO_2.

Unfortunately, we were not able to find the values for $(\mu_{me}(E))_{\text{SiO2}}$ in the literature. Therefore, instead of $(\mu_{me}(E))_{\text{SiO2}}$, we used the mass energy-absorption coefficients of silicon, $(\mu_{me}(E))_{\text{Si}}$, given in Ref. [36]. This difference can be significant for energies less than 100 keV. In Figure 9, the $(\mu_{me}(E))_{\text{Si}}/(\mu_{me}(E))_{\text{air}}$ ratio in terms of beam energy is shown. If we compare the results from Figure 9 with the results from Figure 8, it can be concluded that they do not agree. Namely, on the basis of Figure 9, the sensitivity is expected to decrease with the mean X-ray energy in considered range from 32.57 to 56.70 keV. The reason for this discrepancy between the results from Figures 8 and 9 may lie in the fact that either $(\mu_{me}(E))_{\text{Si}}$ coefficients for silicon are not suitable to be used for SiO_2 or/and the mean energy is not a true indicator of the X-ray beam.
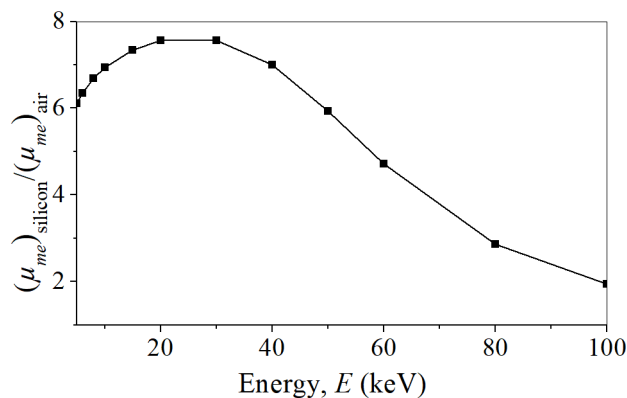

Figure 9. $(\mu_{me}(E))_{\text{silicon}}/(\mu_{me}(E))_{\text{air}}$ ratio versus X-ray photon energy.

Another characteristic of dosimeters, in addition to sensitivity, is fading, f. This shows the recovery of the transistor threshold voltage after irradiation, during annealing at room temperature without gate polarization (so-called spontaneous annealing, SA). The fading can be found as [34]

$$f = \frac{V_T(0) - V_T(t)}{V_T(0) - V_{T0}} = \frac{\Delta V_T(0) - \Delta V_T(t)}{\Delta V_T(0)}, \tag{11}$$

where $V_T(0)$ is the threshold voltage after irradiation, i.e., at the beginning of SA; $V_T(t)$ is the threshold voltage during SA; V_{T0} is the threshold voltage before irradiation; $\Delta V_T(0)$ is the threshold voltage shift after irradiation, i.e., at the beginning of SA; and $\Delta V_T(t)$ is the threshold voltage shift during SA. During SA after gamma irradiation, $\Delta V_T(t)$ usually decreases, which gives the positive fading that increases [34]. Otherwise, $\Delta V_T(t)$ can also increase (reverse annealing), giving the negative fading. Figure 10 shows that the obtained fading is negative for all samples, which is opposite to the case of gamma radiation.
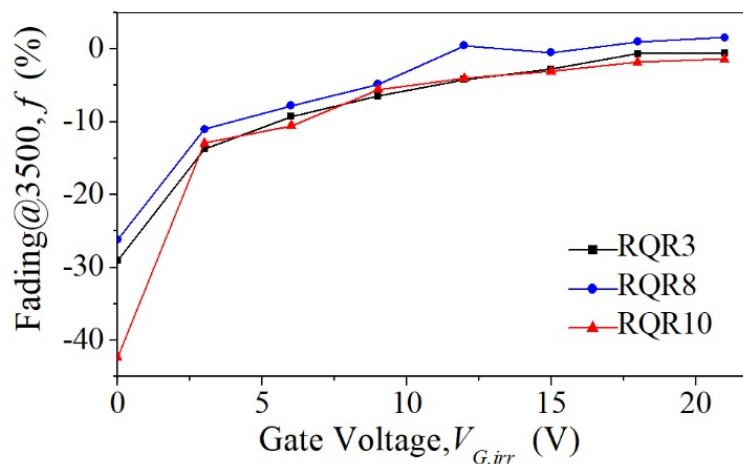

Figure 10. Fading at 3500 h versus gate voltage during irradiation.

Looking at Figures 3 and 10, it cannot be concluded which transistor has the best dosimetric characteristics. Since the sensitivity and fading are the only dosimetric parameters, we introduce a new dosimetric parameter, *Golden Ratio*, *GR*, that connects these two parameters:

$$GR = \frac{S}{f(t_{max})}, \tag{12}$$

where S is the sensitivity and $f(t_{max})$ is the fading at the last point of SA (in our case, $t_{max} \approx 3500$ h, i.e., about 5 months). The higher *GR* represents better dosimetric characteristics of the transistor that should have a large S and a small f (*GR* should be as high as possible). This means that *GR* can be used as a good parameter to compare different transistors or to examine the effect of operating conditions (e.g., as in our case, different gate voltages). The *GR* is displayed in Figure 11, showing that the highest *GR* (the best dosimetric characteristic) is for RQR8 and $V_{G,rad}$ = 12 and 15 V.
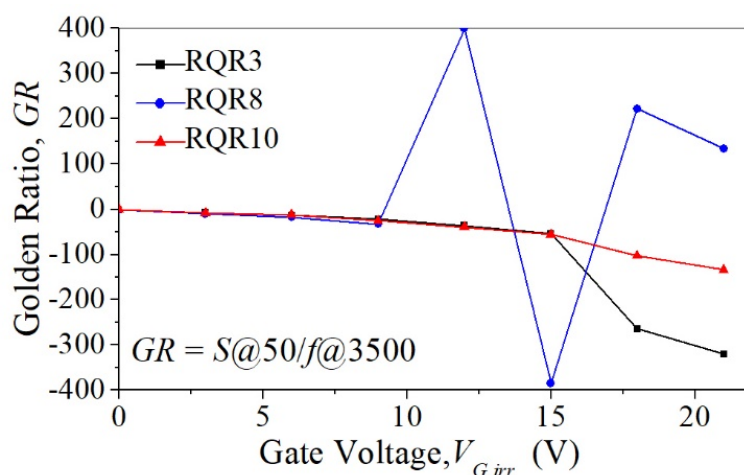
Figure 11. ΔN_{st} at K_{air} = 50 Gy versus gate voltage during irradiation.

4. Conclusions

In this case study, the possibility of using commercial p-channel power vertical double-diffused metal-oxide-semiconductor field-effect transistors (VDMOSFETs) as X-ray sensors is investigated. This is important because VDMOSFETs are potentially suitable for radiation dosimetry because they have a relatively thick oxide. The results show that the $\Delta V_T = f(K_{air})$ dependence of threshold voltage shift, ΔV_T, on air kerma, K_{air}, is linear up to the used air kerma of 50 Gy for all used gate polarizations. The *r*-square (r^2) correlation coefficients of linear regression are higher than 0.99 for all cases. The fitting of dependence of the sensitivity, *S*, on the gate polarization, $V_{G,irr}$, applied during irradiation and using the proposed equation is good. The density of FTs, ΔN_{ft}, is the highest for RQR8 but the lowest for the RQR3 beam. The density of STs, ΔN_{st}, does not show any clear dependence on $V_{G,irr}$ as ΔN_{ft}. ΔN_{ft} is two times higher than ΔN_{st}, having a more dominant effect on ΔV_T than ΔN_{st}. However, the effect of STs on ΔV_T is more significant than in the case of gamma-radiation, where ΔN_{ft} is usually more than five times higher than ΔN_{st}. The mass energy-absorption coefficients for silicon-dioxide, $(\mu_{me}(E))_{SiO2}$, have not been found in the literature, and the mass energy-absorption coefficients for silicon, $(\mu_{me}(E))_{Si}$, are used for ΔN_{ft} on K_{air} dependence explanation. However, there is a discrepancy between the experimental results and theoretical predictions. As a consequence, either the $(\mu_{me}(E))_{Si}$ coefficients for silicon are not suitable to be used for SiO_2 and/or the mean energy is not a proper indicator of the X-ray beam. All transistors show the negative fading during spontaneous annealing, which is not the case with gamma-radiation. The newly proposed dosimetry parameter, called the Golden Ratio, *GR*, is a very useful tool for comparing different dosimeter conditions.

Author Contributions: Conceptualization, G.S.R.; validation, G.S.R., S.D.I.; A.J.P., and M.S.A.; investigation, G.S.R., S.V., A.S.J., S.D. and S.S.; writing—original draft preparation, G.S.R. All authors have read and agreed to the published version of the manuscript.

Data Availability Statement: Not applicable.

References

1. Holmes-Siedle, A. The space-charge dosimeter: General principles of a new method of radiation detection. *Nucl. Instrum. Methods* **1974**, *121*, 169–179. [CrossRef]
2. Danković, D.; Mitrović, N.; Prijić, Z.; Stojadinović, N.D. Modeling of NBTS effects in p-channel power VDMOSFETs. *IEEE Trans. Device Mater. Reliab.* **2020**, *20*, 204–213. [CrossRef]
3. Sezgin-Ugranlı, H.G.; Özçelep, Y. Determination of power MOSFET's gate oxide degradation under different electrical stress levels based on stress-induced oxide capacitance changes. *IEEE Trans. Electron Devices* **2021**, *68*, 688–696. [CrossRef]
4. Abubakkar, S.F.O.; Zabah, N.F.; Abdullah, Y.; Fauzi, D.A.; Muridan, N.; Hasbullah, N.F. Effects of electron radiation on commercial power MOSFET with buck converter application. *Nucl. Sci. Tech.* **2017**, *28*, 31. [CrossRef]
5. Lebedev, A.A.; Levinshtein, M.E.; Ivanov, P.A.; Kozlovski, V.V.; Strel'chuk, A.M.; Shabunina, E.I.; Fursin, L. Effect of irradiation with 15-MeV protons on low frequency noise in power SiC MOSFETs. *Semiconductors* **2019**, *53*, 1568–1572. [CrossRef]
6. Abbate, C.; Busatto, G.; Tedesco, D.; Sanseverino, A.; Silvestrin, L.; Velardi, F.; Wyss, J. Gate damages induced in SiC power MOSFETs during heavy-ion irradiation—Part I. *IEEE Trans. Electron Devices* **2019**, *66*, 4235–4242. [CrossRef]
7. Sun, Y.; Wang, T.; Liu, Z.; Xu, J. Investigation of irradiation effects and model parameter extraction for VDMOS field effect transistor exposed to gamma rays. *Radiat. Phys. Chem.* **2021**, *185*, 109478. [CrossRef]
8. Zeng, G.; Liu, X.; Yang, G.; Li, L.; Chen, X.; Jian, Z.; Zhu, S.; Pang, Y. Investigation on γ radiation effects of N-channel VDMOSFETs irradiated without electric field stress. *Microelectron. Reliab.* **2021**, *116*, 114019. [CrossRef]
9. Assaf, J. Characterization of commercial p-MOSFETs for using as a gamma-rays dosimeter. *Silicon* **2022**, *14*, 1767–1774. [CrossRef]
10. Farroh, H.A.; Nasr, A.; Sharshar, K.A. A Study of the performance of an n-channel MOSFET under gamma radiation as a dosimeter. *J. Electron. Mater.* **2020**, *49*, 5762–5772. [CrossRef]
11. Pejovic, M.M. Application of p-channel power VDMOSFET as a high radiation doses sensor. *IEEE Trans. Nucl. Sci.* **2015**, *62*, 1905–1910. [CrossRef]
12. Wang, T.; Wan, X.; Jin, H.; Li, H.; Sun, Y.; Liang, R.; Xu, J.; Zheng, L. Optimization of the cell structure for radiation-hardened power MOSFETs. *Electronics* **2019**, *8*, 598. [CrossRef]
13. Abunahla, H.; Mohammad, B. Memristor device for security and radiation applications. In *Memristor Technology: Synthesis and Modeling for Sensing and Security Applications. Analog Circuits and Signal Processing*; Springer: Cham, Switzerland, 2015; pp. 75–92. [CrossRef]
14. Bessia, F.A.; Flandre, D.; André, N.; Irazoqui, J.; Pérez, M.; Berisso, M.G.; Lipovetzky, J. Fully-depleted SOI MOSFET sensors in accumulation mode for total dose measurement. In Proceedings of the 2018 IEEE Nuclear Science Symposium and Medical Imaging Conference (NSS/MIC), Sydney, Australia, 10–17 November 2018; pp. 1–3. [CrossRef]
15. Bibilashvili, A.; Kushitashvili, Z. Radiation effect on the parameters of field effect transistors with Schottky barrier on GaAs. *IOP Conf. Ser. Earth Environ. Sci.* **2019**, *362*, 012071. [CrossRef]
16. Di Bartolomeo, A.; Urban, F.; Pelella, A.; Grillo, A.; Passacantando, M.; Liu, X.; Giubileo, F. Electron irradiation of multilayer PdSe2 field effect transistors. *Nanotechnology* **2020**, *31*, 375204. [CrossRef] [PubMed]
17. Kahraman, A.; Deevi, S.C.; Yilmaz, E. Influence of frequency and gamma irradiation on the electrical characteristics of Er_2O_3, Gd_2O_3, Yb_2O_3, and HfO_2 MOS-based devices. *J. Mater. Sci.* **2020**, *55*, 7999–8040. [CrossRef]
18. Manikanthababu, N.; Basu, T.; Vajandar, S.; Rao, S.V.S.N.; Panigrahi, B.K.; Osipowicz, T.; Pathak, A.P. Radiation tolerance, charge trapping, and defect dynamics studies of ALD-grown $Al/HfO_2/Si$ nMOSCAPs. *J. Mater. Sci. Mater. Electron.* **2020**, *31*, 3312–3322. [CrossRef]
19. Sharma, C.; Singh, R.; Chao, D.S.; Wu, T.L. Effects of γ-Ray irradiation on AlGaN/GaN heterostructures and high electron mobility transistor devices. *J. Electron. Mater.* **2020**, *49*, 6789–6797. [CrossRef]
20. Vikulin, I.M.; Gorbachev, V.E.; Nazarenko, A.A. Radiation sensitive detector based on field-effect transistors. *Radioelectron. Commun. Syst.* **2017**, *60*, 401–404. [CrossRef]
21. Carvajal, M.A.; Escobedo, P.; Jiménez-Melguizo, M.; Martínez-García, M.S.; Martínez-Martí, F.; Martínez-Olmos, A.; Palma, A.J. A compact dosimetric system for MOSFETs based on passive NFC tag and smartphone. *Sens. Actuators A* **2017**, *267*, 82–89. [CrossRef]
22. Li, X.; Yang, J.; Liu, C. A technique for characterizing ionization and displacement defects in NPN transistors induced by 1-MeV electron irradiation. *IEEE Trans. Nucl. Sci.* **2018**, *65*, 539–544. [CrossRef]
23. Prakash, A.P.G.; Pradeep, T.M.; Hegde, V.N.; Pushpa, N.; Bajpai, P.K.; Patel, S.P.; Trivedi, T.; Bhushan, K.G. Comparison of effect of 5 MeV proton and Co-60 gamma irradiation on silicon NPN rf power transistors and N–channel depletion MOSFETs. *Radiat. Eff. Defects Solids* **2017**, *172*, 952–963. [CrossRef]
24. Anjum, A.; Pradeep, T.M.; Vinayakprasanna, N.H.; Pushpa, N.; Tripathi, A.; Prakash, A.P.G. Analysis of 80-MeV carbon and 80-MeV nitrogen ion irradiation effects on n-channel MOSFETs. *IEEE Trans. Device Mater. Reliab.* **2019**, *19*, 696–703. [CrossRef]
25. Tai, Y.; Yeh, S.; Huang, S.; Chang, T. Total-dose effect of X-ray irradiation on low-temperature polycrystalline silicon thin-film transistors. *IEEE Electron Device Lett.* **2020**, *41*, 864–867. [CrossRef]
26. Ristić, G.S.; Jevtić, A.S.; Ilić, S.D.; Dimitrijević, S.; Veljković, S.; Palma, A.J.; Stanković, S.; Andjelković, M.S. Sensitivity of unbiased commercial p-channel power VDMOSFETs to X-ray radiation. In Proceedings of the IEEE 32nd International Conference on Microelectronics (MIEL 2021), Nis, Serbia, 12–14 September 2021; pp. 341–344. [CrossRef]

27. Zhang, C.-M.; Jazaeri, F.; Borghello, G.; Mattiazzo, S.; Baschirotto, A.; Enz, C. A generalized EKV charge-based MOSFET model including oxide and interface traps. *Solid-State Electron.* **2021**, *177*, 107951. [CrossRef]

28. Miyoshi, Y.; Ishikawa, K.; Sekine, M.; Hori, M.; Tatsumi, T. Reduction in photon-induced interface defects by optimal pulse repetition rate in the pulse-modulated inductively coupled plasma. *Jpn. J. Appl. Phys.* **2021**, *60*, 010906. [CrossRef]

29. Poludniowski, G.; Landry, G.; De Blois, F.; Evans, P.M.; Verhaege, F. SpekCalc: A program to calculate photon spectra from tungsten anode x-ray tubes. *Phys. Med. Biol.* **2009**, *54*, N433–N438. [CrossRef]

30. Ilić, S.; Jevtić, A.; Stanković, S.; Ristić, G. Floating-gate MOS transistor with dynamic biasing as a radiation sensor. *Sensors* **2020**, *20*, 3329. [CrossRef]

31. Ristić, G.S. Influence of ionizing radiation and hot carrier injection on metal-oxide-semiconductor transistors. *J. Phys. D Appl. Phys.* **2008**, *41*, 023001. [CrossRef]

32. McWhorter, P.J.; Winokur, P.S. Simple technique for separating the effects of interface traps and trapped-oxide charge in metal-oxide-semiconductor transistors. *Appl. Phys. Lett.* **1986**, *48*, 133–135. [CrossRef]

33. Ristic, G.S.; Andjelkovic, M.S.; Jaksic, A.B. The behavior of fixed and switching oxide traps of RADFETs during irradiation up to high absorbed doses. *Appl. Radiat. Isot.* **2015**, *102*, 29–34. [CrossRef]

34. Ristic, G.S.; Ilic, S.D.; Duane, R.; Andjelkovic, M.S.; Palma, A.J.; Lallena, A.M.; Krstic, M.D.; Stankovic, S.J.; Jaksic, A.B. Radiation sensitive MOSFETs irradiated with various positive gate biases. *J. Radiat. Res. Appl. Sci.* **2021**, *14*, 353–357. [CrossRef]

35. Ristić, G.S.; Pejović, M.M.; Jakšić, A.B. Comparison between post-irradiation annealing and post-high electric field stress annealing of n-channel power VDMOSFETs. *Appl. Surf. Sci.* **2003**, *220*, 181–185. [CrossRef]

36. Hubbell, J.H.; Seltzer, S.M. X-Ray Mass Attenuation Coefficients. Available online: http://physics.nist.gov/xaamdi (accessed on 13 December 2021).